

# Poly (*N*-Isopropylacrylamide) Microgel-Based Optical Devices for Humidity Sensing

Molla R. Islam, Shuyi Xie, Danqing Huang, Keady Smyth and Michael J. Serpe\*

Department of Chemistry, University of Alberta, Edmonton, AB, T6G 2G2

\*Corresponding Author: Michael J. Serpe (michael.serpe@ualberta.ca)

## **Abstract:**

Optical sensors for environmental humidity have been constructed from poly (*N*-isopropylacrylamide)-*co*-acrylic acid (pNIPAm-*co*-AAc) microgels. The devices were constructed by first depositing a monolithic layer of pNIPAm-*co*-AAc microgels on a Au-coated glass substrate followed by the addition of another Au layer on top. The resultant assembly showed visual color, and exhibited multiplexed reflectance spectra. We found that the thickness of the device's microgel layer depended on environmental humidity, which corresponded to a change in the device's optical properties. Specifically, at low humidity the microgel layer was collapsed, while it absorbed water from the atmosphere (and swelled) as the humidity increased. Additionally, we investigated how the deposition of the hygroscopic polymer poly (diallyldimethylammonium chloride) (pDADMAC) onto the microgel layer (prior to final Au layer deposition) influenced the device's humidity response. We found that the devices were more sensitive to humidity as the number of pDADMAC layers in the device increased. Finally, we evaluated the

device performance at various temperatures, and found that the sensitivity was enhanced at low temperature, although the response was more linear at elevated temperature.

**Keywords:** Optical sensing, Humidity sensing, Photonic materials, Stimuli responsive polymers, Poly (N-isopropylacrylamide)-based microgels

## **Introduction:**

For decades, polymeric materials have proven to be an important (if not the most important) class of materials for myriad applications. This is mainly due to the versatility of their synthesis and facile chemical modification to yield materials with tailor-made mechanical properties, morphologies, and function.[1, 2] While polymers themselves are interesting, perhaps even more interesting are materials that can "sense" and "respond" to their environment by changing their chemical and/or physical properties.[3] Polymers with this ability are referred to as stimuli responsive (or smart) polymers, and have found numerous applications[4-11] as a result of their response to stimuli like pH, temperature, concentration, presence of analytes, and electric/magnetic fields.[12-17] Ideally, the response of the polymers should be fully reversible once the environmental stimulus is removed.

One of the most extensively studied stimuli responsive polymers is poly (*N*-isopropylacrylamide) (pNIPAm).[18-22] PNIPAm is a thermoresponsive polymer that undergoes a conformational change from an extended coil to compact globule in water when the temperature is raised  $> 32\text{ }^{\circ}\text{C}$ , which is pNIPAm's lower critical solution temperature (LCST).[23] Above this temperature, pNIPAm transitions from a hydrophilic to a relatively hydrophobic state, where polymer-polymer interactions dominate. Additionally, crosslinked networks of pNIPAm (hydrogels) and colloidally stable hydrogel particles (microgels) can be synthesized. Like their linear counterparts, pNIPAm-based hydrogels and microgels are thermoresponsive; they decrease in size at elevated temperature, while they swell at low temperature. PNIPAm-based materials can

also be made responsive to a number of stimuli by incorporation of additional functional groups at the time on synthesis. The most common functionalities added are amines and/or carboxylic acids; for example, acrylic acid (AAc), methacrylic acid (MAAc), vinyl acetic acid and N-(3-Aminopropyl) methacrylamide hydrochloride (APMAH).[12-14, 24-26] In previous work, we showed that optical devices could be fabricated by sandwiching pNIPAm-based microgels between two Au layers supported on a glass substrate. This device, referred to as an etalon, exhibits visible color and multiplex reflectance spectra as shown in Figure 1. The position of the peaks in the reflectance spectra depends on a number of factors according to equation (1):[27]

$$\lambda = (2nd \cos \theta) / m \quad (1)$$

where n is the refractive index of the microgel (dielectric) layer, d is the mirror-mirror distance,  $\theta$  is the angle of incident light relative to the device normal, and m (an integer) is the order of the spectral peak. We point out that while the device's optical properties depend on the parameters in equation (1), the mirror-mirror distance is primarily responsible for the tunable optical properties of our devices (at a single observation angle).

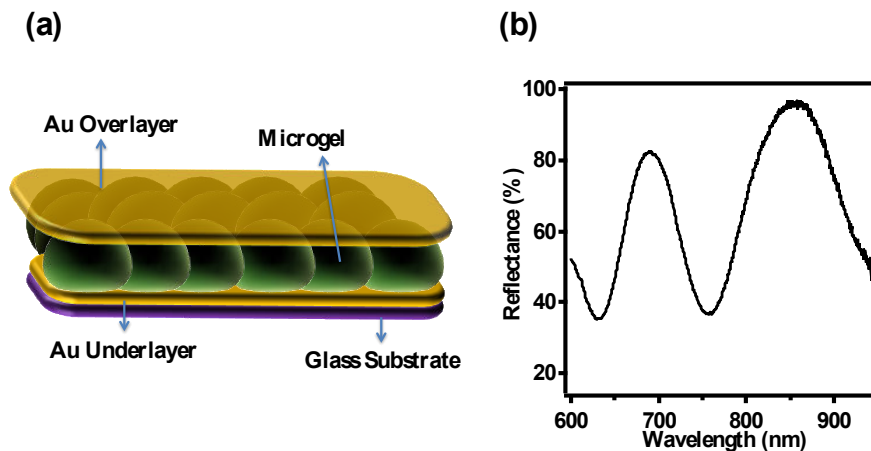


Figure 1: (a) Schematic of a microgel-based etalon. (b) A typical reflectance

spectrum of a pNIPAm-*co*-AAc microgel-based etalon.

We have used pNIPAm-*co*-AAc microgels and microgel-based etalons for many applications, such as: for sensing and biosensing, artificial muscles, water remediation and drug delivery.[15, 28-34] To expand the scope and utility of etalons, we show here that humidity responsive microgel-based etalons can be fabricated, and their sensitivity to humidity enhanced by depositing a hygroscopic polyelectrolyte layer before deposition of the final Au layer.[35, 36] Specifically, the devices were fabricated by depositing a polycationic poly (diallyldimethylammonium chloride) (pDADMAC) layer on top of the pNIPAm-*co*-AAc (polyanionic) microgel layer that was painted on a Cr/Au coated glass substrate. The final devices were achieved by depositing another Cr/Au layer on the polymer layers. Additional devices were fabricated by depositing a layer of polyanionic poly (sodium 4-styrenesulfonate) (PSS) on the first pDADMAC layer, followed by addition of another pDADMAC layer prior to the deposition of the final Cr/Au layer. These layers were strongly bound to each other (and subsequently to the substrate) via electrostatic interactions. Finally, additional devices were fabricated by depositing another layer of PSS and pDADMAC onto the existing layers prior to the final Cr/Au layer deposition.[37] Once the devices were constructed, we investigated their response to humidity. We found that the number of multilayers deposited on the initial microgel layer significantly improves the sensitivity of the devices to changes in environmental humidity, which was attributed to increased water affinity for devices with increased layers of the hygroscopic pDADMAC. We also found that temperature influences the device's performance, which we attributed to the pNIPAm thermoresponsivity.

## **Experimental:**

**Materials:** N,N'-methylenebisacrylamide (BIS) (99%), acrylic acid (AAc) (99%), and ammonium persulfate (APS) (98+%) were obtained from Sigma-Aldrich (Oakville, Ontario), poly(sodium 4-styrene-sulfonate) (PSS) and poly (diallyldimethylammonium chloride) solution (pDADMAC) of MW <100,000 (20% in water) was purchased from Sigma-Aldrich (St. Louis, MO) and were used as received. *N*-Isopropylacrylamide (NIPAm) was purchased from TCI (Portland, Oregon) and purified by recrystallization from hexanes (ACS reagent grade, EMD, Gibbstown, NJ) prior to use. Deionized (DI) water with a resistivity of 18.2 M $\Omega$ •cm was used. Fisher's finest glass coverslips were 25×25 mm and obtained from Fisher Scientific (Ottawa, Ontario). Cr was 99.999% and obtained from ESPI (Ashland, OR), while Au was 99.99% and obtained from MRCS Canada (Edmonton, AB). Anhydrous ethanol was obtained from Commercial Alcohols (Brampton, Ontario). Annealing of the Au-Cr coated cover slips was done in a Thermolyne muffle furnace from Thermo Fisher Scientific (Ottawa, Ontario).

### **Poly (*N*-isopropylacrylamide)-*co*-acrylic acid Microgel Synthesis:**

Poly (*N*-isopropylacrylamide)-*co*-acrylic acid (pNIPAm-*co*-AAc) microgels were synthesized via temperature-ramp, surfactant free, free radical precipitation polymerization as described previously.[26] The pregel solution was comprised of 85% (mole/mole) NIPAm, 10% AAc, and 5% BIS as the crosslinker. Initially, NIPAm (17.0 mmol), and BIS (1.0 mmol) were dissolved in deionized water (100 mL) with stirring in a beaker. The mixture was filtered through a 0.2  $\mu$ m syringe filter affixed to a 20 mL syringe into a 200 mL 3-neck round-bottom flask. The beaker was rinsed with 25 mL of deionized water, filtered and added to the NIPAm/BIS solution. The round bottom flask

was then equipped with a temperature probe, a condenser and a N<sub>2</sub> gas inlet. The solution was bubbled with N<sub>2</sub> gas for ~1.5 h, while stirring at a rate of 450 RPM, allowing the temperature to reach 45 °C. AAc (2.0 mmol) was then added to the heated mixture with a micropipette in one aliquot. A 0.078 M aqueous solution of APS (5 mL) was delivered to the reaction flask with a transfer pipet to initiate the reaction. Immediately following initiation, a temperature ramp of 45 to 65 °C was applied to the solution at a rate of 30 °C/h. The reaction was allowed to proceed overnight at 65 °C. After polymerization, the reaction mixture was allowed to cool to room temperature and filtered through glass wool to remove any large aggregates. The coagulum was rinsed with deionized water and filtered through glass wool. Aliquots of these microgel solution (14 mL) were centrifuged at a speed of ~8500 relative centrifugal force (RCF) at 23 °C for ~ 45 minutes to produce a pellet at the bottom of the centrifuge tube. The supernatant was removed from the pellet of microgels. The pellet of microgels was then resuspended with deionized water to the original volume (14 mL). This process was repeated a total of six times to remove any unreacted monomer and/or linear polymer from the microgel solution. This concentrated microgel was used to fabricate the devices. The diameter of the microgel particles was measured to be  $\approx 1.5 \mu\text{m}$  by a differential interference contrast microscope (data not shown).

### **Device Fabrication:**

Pre-cleaned glass cover slips (2.54 cm<sup>2</sup>) were rinsed with DI water and ethanol and dried with N<sub>2</sub> gas, and 2 nm of Cr followed by 15 nm of Au were thermally evaporated onto them at a rate of  $\sim 0.2 \text{ \AA s}^{-1}$  and  $\sim 0.1 \text{ \AA s}^{-1}$ , respectively, using a Torr International Inc. model THEUPG thermal evaporation system (New Windsor, NY). The Cr acts as

adhesion layer to hold the Au layer on the substrate. A concentrated solution of microgels (from centrifugation) was vortexed and placed onto a hot plate at 30 °C. An aliquot (40  $\mu\text{L}$  for each 2.54  $\text{cm}^2$ ) of the concentrated microgels was added to a Au-coated glass substrate (also on a hot plate held at 30 °C) and then spread toward each edge using the side of a micropipette tip according to our previously reported protocol.[38] The substrate was rotated, and the microgel solution was spread again to avoid uneven drying. The spreading and rotation continued until the microgel solution became too viscous to spread due to drying. The microgel solution was allowed to dry completely on the substrate for 2 h with the hot plate temperature set to 35 °C. After 2 h, the dry film was rinsed copiously with DI water to remove any excess microgels not bound directly to the Au. The microgel coated substrate was then placed into a DI water bath and allowed to incubate overnight on a hot plate set to  $\sim 30$  °C. Following this step, the substrate was again rinsed with DI water to further remove any microgels not bound directly to the Au surface. The microgel-coated substrate was then dried with  $\text{N}_2$  gas. Some of the microgel painted substrates were subsequently coated with another layer of Cr/Au to complete the etalon fabrication. Other devices were further exposed to pDADMAC solution (2 mg/mL, pH = 6.5) and PSS solution (2 mg/mL, pH= 4.35) to yield the desired layers on top of the microgels. Each layer was deposited by dipping substrates in the respective solutions, with copiously washing with DI water and drying between layer depositions. In this study, we deposited a single pDADMAC layer on top of the microgel layer prior to final Au layer deposition; devices composed of pDADMAC/PSS/pDADMAC and pDADMAC/PSS/pDADMAC/PSS/pDADMAC were also constructed, as shown schematically in Figure 2.

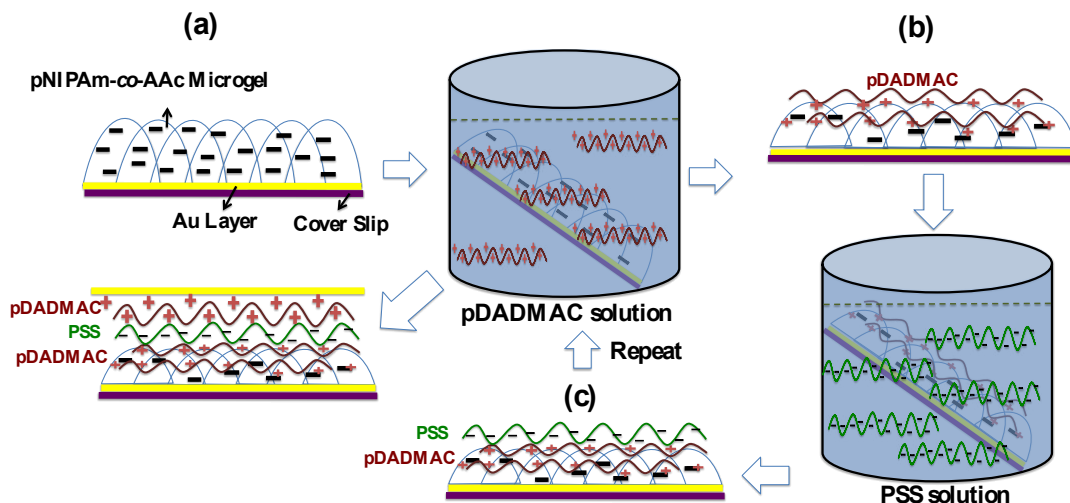


Figure 2: Schematic of humidity-responsive device fabrication. (a) PNIPAm-co-AAc microgel-coated substrates can either be coated with a final Au layer to complete device fabrication, or subsequent polymer layers can be deposited on the microgel layer prior to final Au deposition. (b) A pDADMAC layer can be deposited on the microgel layer by dipping the substrate into a pDADMAC solution, followed by rinsing and coating with the final Au layer. Alternatively, another pDADMAC layer can be added to the device by first adding a layer of (c) PSS, rinsing, and exposing the substrate to pDADMAC once again and depositing Au. This process can be repeated any number of times prior to Au layer deposition.

### Humidity Response:

The devices were fixed in the center of a sealed chamber fitted with a humidity feedback system by ramé-hart Instrument Co. (Model 100-26 TH) that was capable of controlling humidity using an Air-O-Swiss AOS 7145 Cool Mist Ultrasonic humidifier (manufactured by Swiss Pure Air) and a humidity sensor from TEGAM (Model RDP-

20C). Reflectance spectra were collected using a USB2000+ spectrophotometer, a HL-2000-FHSA tungsten light source, and a R400-7-VIS-NIR optical fiber reflectance probe all from Ocean Optics (Dunedin, FL) and positioning the light source above the center of the devices. The distance between the reflectance probe and the devices was adjusted to yield optimal reflectance spectra, and was typically 0.2-0.3 cm. The distance was unchanged in each experiment. Spectra were recorded using Ocean Optics Spectra Suite Spectroscopy Software over a wavelength range of 350–1025 nm. A digital temperature controller was connected to the chamber, which allowed us to control the temperature of the chamber. Reflectance spectra were collected at various humidities and temperatures using this setup — one full humidity increase/decrease cycle typically took 4 hr.

### **Results and Discussion:**

Initial experiments focused on determining the response of unmodified microgel-based etalons to changes in humidity at various temperatures, and the results can be seen in Figure 3. As can be seen, at all temperatures, the  $\lambda_{\text{max}}$  of the reflectance peak shifts

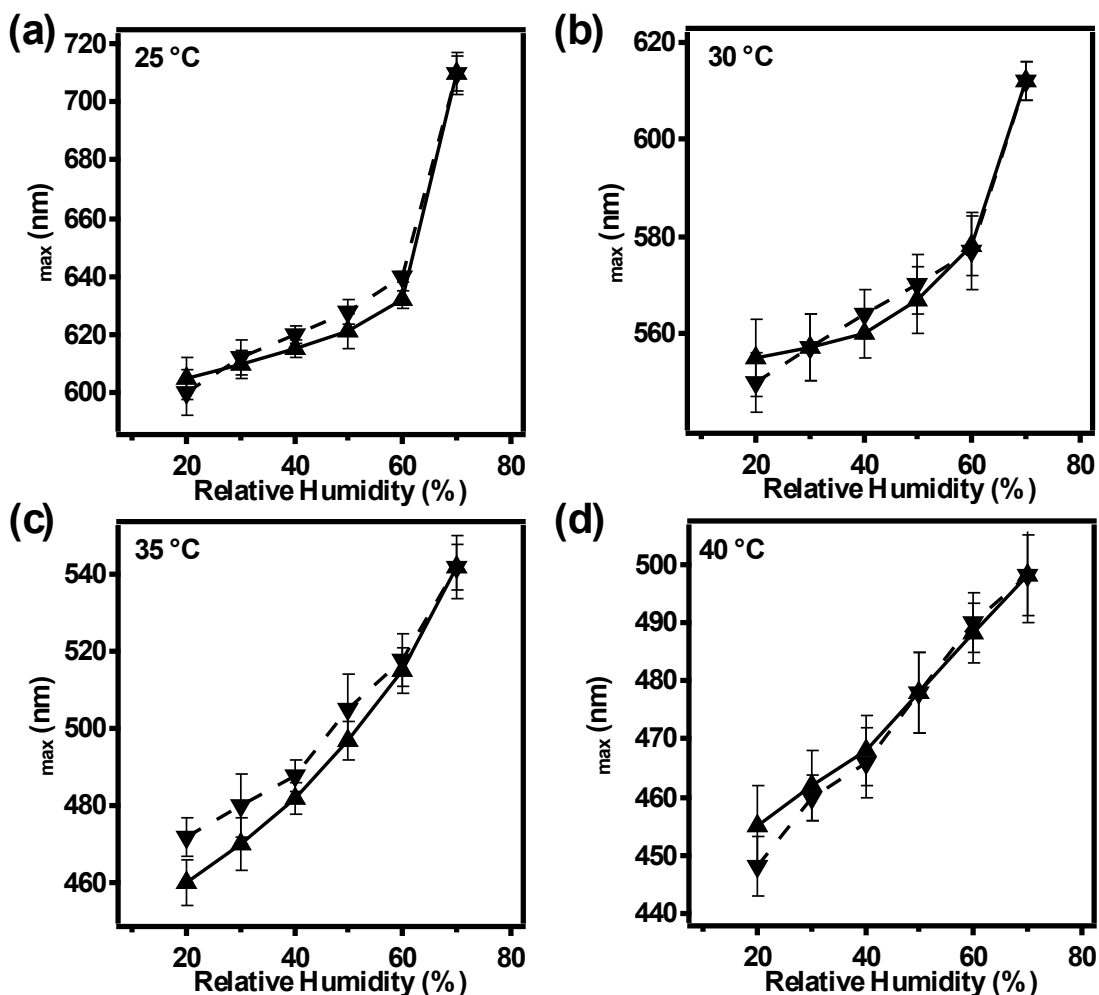


Fig 3. Position of a single reflectance peak ( $\lambda_{\max}$ ) for devices at (a) 25 °C, (b) 30 °C, (c) 35 °C, and (d) 40 °C. Here, symbol (▲) indicates a humidity increase cycle while symbol (▼) denotes a humidity decrease cycle. Each data point represents the average of at least three independent measurements on the same device, and the error bars are the standard deviation for those values.

to higher values as the humidity increased. We hypothesize that this is a result of the air moisture partitioning into (and swelling) the hygroscopic microgel layer of the device, leading to an increased mirror-mirror distance, and a concomitant red shift, according to

equation 1.[39] With decreasing humidity the  $\lambda_{\max}$  of the spectral peaks shift toward lower wavelength (blue shift), which we hypothesize is due to the microgel layer desolvating, leading to a decrease in the distance between the etalon's mirrors. We also note that the hysteresis between humidity increase/decrease cycles is minimal. As can be seen in Figure 3 (a,b), when the etalons are held at  $T < LCST$ , there is a sharp increase in  $\lambda_{\max}$  at 60% humidity. We attribute this to the relatively hydrophilic nature of pNIPAm at this temperature, allowing the device to become fully water saturated at this humidity. For comparison, the data in Figure 3 (c,d) show that this sharp increase was not observed at  $T > LCST$ , and the response is more linear over a larger humidity range. The humidity response can be repeated with the same device over many cycles, as can be seen in Figure 4(a), making these devices useful for sensing atmospheric humidity.

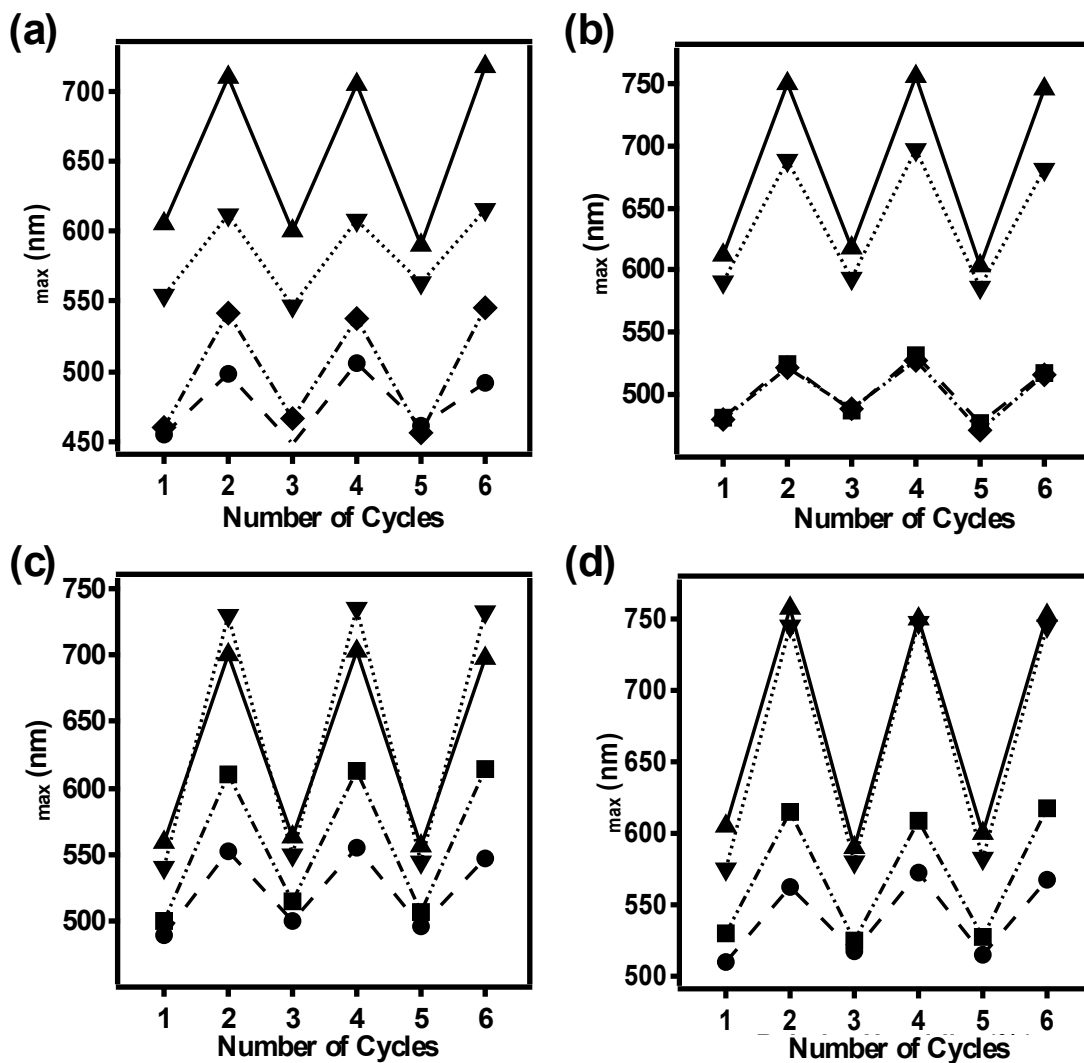


Fig 4. Position of a single reflectance peak ( $\lambda_{\max}$ ) for an (a) etalon, (b) etalon with a single pDADMAC layer, (c) an etalon with layers pDADMAC/PSS/pDADMAC, and (d) an etalon with layers pDADMAC/PSS/pDADMAC/PSS/pDADMAC. We point out that the layers are deposited on the microgels prior to final Au deposition. The experiments were conducted at (▲) 25 °C, (▼) 30 °C, (■) 35 °C, and (●) 40 °C and the humidity cycled between (odd numbers) 20 and (even numbers) 70 % on the same device.

In an effort to make the devices more sensitive to humidity, we modified the microgel layers with hygroscopic polymers. We hypothesized that if we could render the microgel layer more hygroscopic it would be able to absorb large amounts of water from the atmosphere (compared to the microgels alone) leading to an enhancement of the device's optical response. In previous studies, we showed that pNIPAm microgel-based layers on surfaces become increasingly hygroscopic upon the addition of the polycation pDADMAC.[37, 39] Inspired by our previous work, microgel-based etalons were fabricated with varying numbers of pDADMAC layers deposited on the microgel layer prior to the addition of the final Au layer on top of the microgel layer. Specifically, the pNIPAm-co-AAc microgel layer was deposited on the Au-coated glass coverslip as usual, then the substrate was dipped into a pDADMAC solution (pH= 6.5) for 20 min, rinsed copiously with DI water, dried and finally coated with the Au overlayer to generate the etalon. Figure 5 shows the response of the etalon composed of a single pDADMAC layer on the microgels to humidity as a function of temperature. As can be seen from Figure 5, we observe that the device are more sensitive at temperature below 32 °C. This may be due to the fact that the microgels are crosslinked by the electrostatic interaction with the pDADMAC. Therefore, the layer between the Au starts off in a relatively collapsed state (compared to just the microgels), while still maintaining its ability (perhaps enhanced ability due to the pDADMAC layer) to absorb atmospheric moisture. Therefore, the response is enhanced compared to the microgels alone. Like the microgel layer alone, the response of the device to humidity became more linear at temperature above 32 °C, while still maintaining minimal hysteresis at all temperatures.

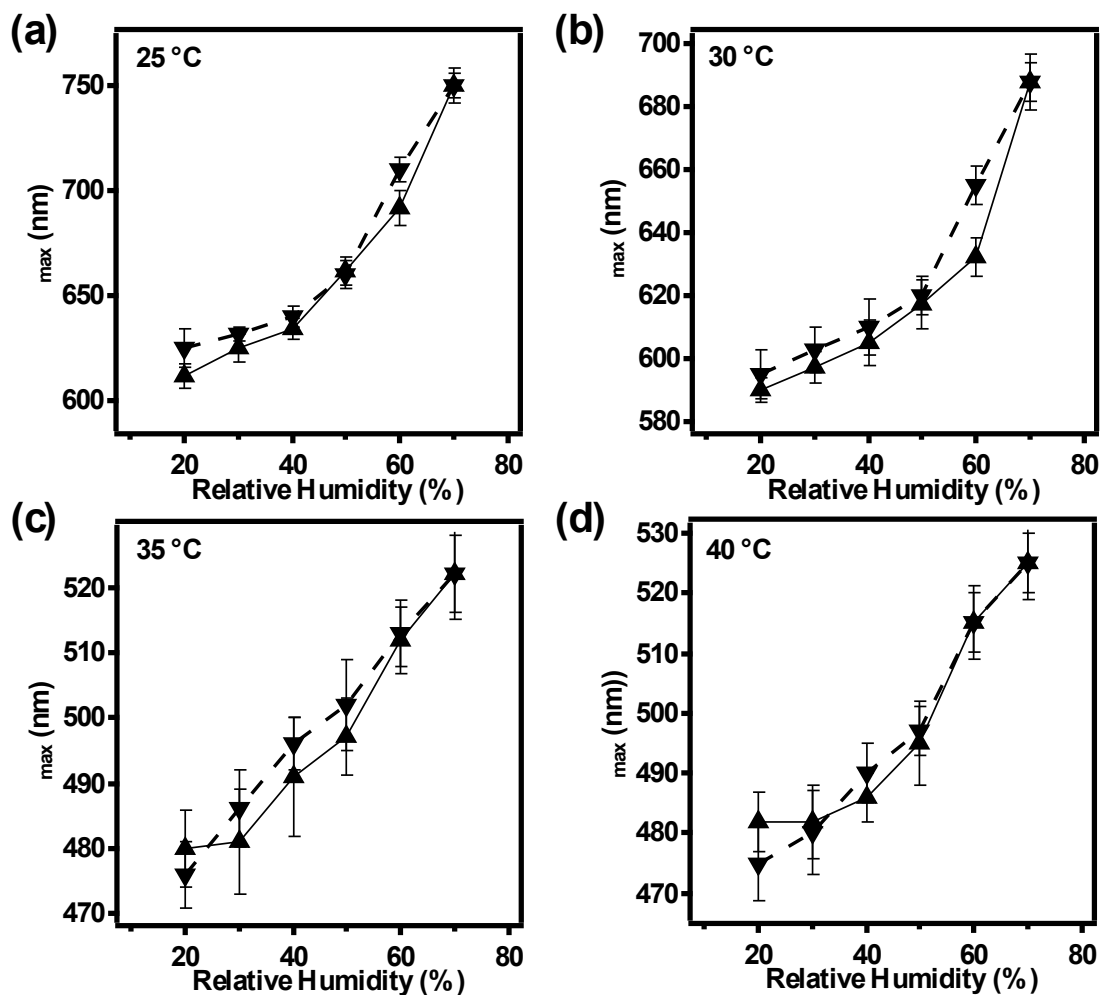


Fig 5. Position of a single reflectance peak ( $\lambda_{\max}$ ) for an etalon composed of microgels with a single pDADMAC layer at (a) 25 °C, (b) 30 °C, (c) 35 °C, and (d) 40 °C. Here, symbol (▲) indicates a humidity increase cycle while symbol (▼) denotes a humidity decrease cycle. Each data point represents the average of at least three independent measurements on the same device, and the error bars are the standard deviation for those values.

Devices coated with 2 pDADMAC layers (pDADMAC/PSS/pDADMAC) and 3 pDADMAC layers (pDADMAC/PSS/pDADMAC/PSS/pDADMAC) on the microgel

layer were also constructed. These multilayer devices were made by sequential addition of pDADMAC and PSS by layer-by-layer (LbL) approach followed by Au overlayer deposition. Firstly, a pDADMAC layer was deposited onto the microgel-coated substrate followed by a PSS layer. Repeating this process yielded the desired devices. The responses for the devices composed of 2 pDADMAC layers and 3 pDADMAC layers are shown in Figures 6 and 7, respectively. Their response to multiple cycles of increased/decreased humidity is shown in Figure 4. As can be seen, the devices composed of pDADMAC/PSS/pDADMAC and pDADMAC/PSS/pDADMAC/PSS/pDADMAC layers exhibit increased sensitivity compared to devices with only a single pDADMAC layer. Similarly, these devices show less sensitivity at temperatures above 32 °C. But the response is again more linear, and has a larger linear range, at high temperature (Figure 6 and Figure 7).

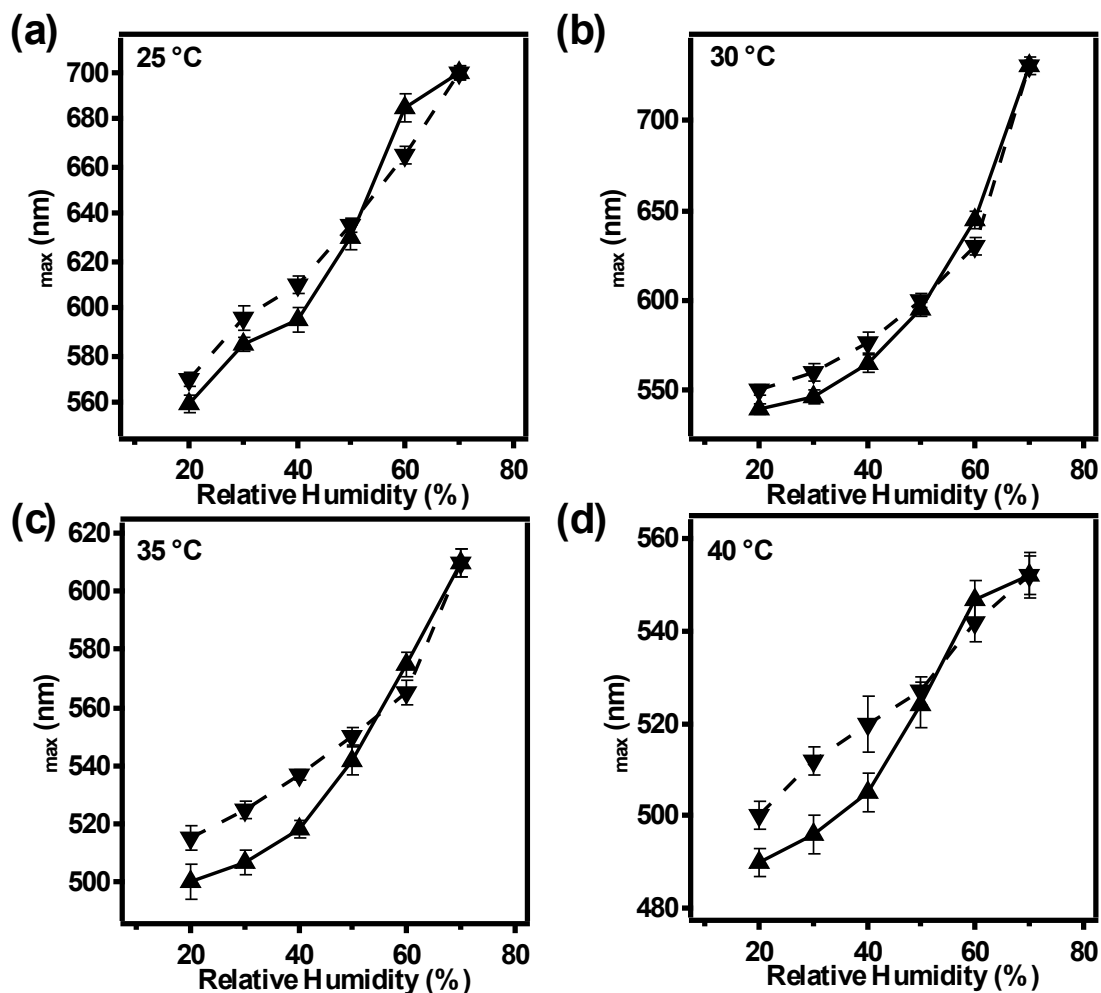


Fig 6. Position of a single reflectance peak ( $\lambda_{\max}$ ) for an etalon composed of microgels coated with pDADMAC/PSS/pDADMAC at (a) 25 °C, (b) 30 °C, (c) 35 °C, and (d) 40 °C. Here, symbol (▲) indicates a humidity increase cycle while symbol (▼) denotes a humidity decrease cycle. Each data point represents the average of at least three independent measurements on the same device, and the error bars are the standard deviation for those values.

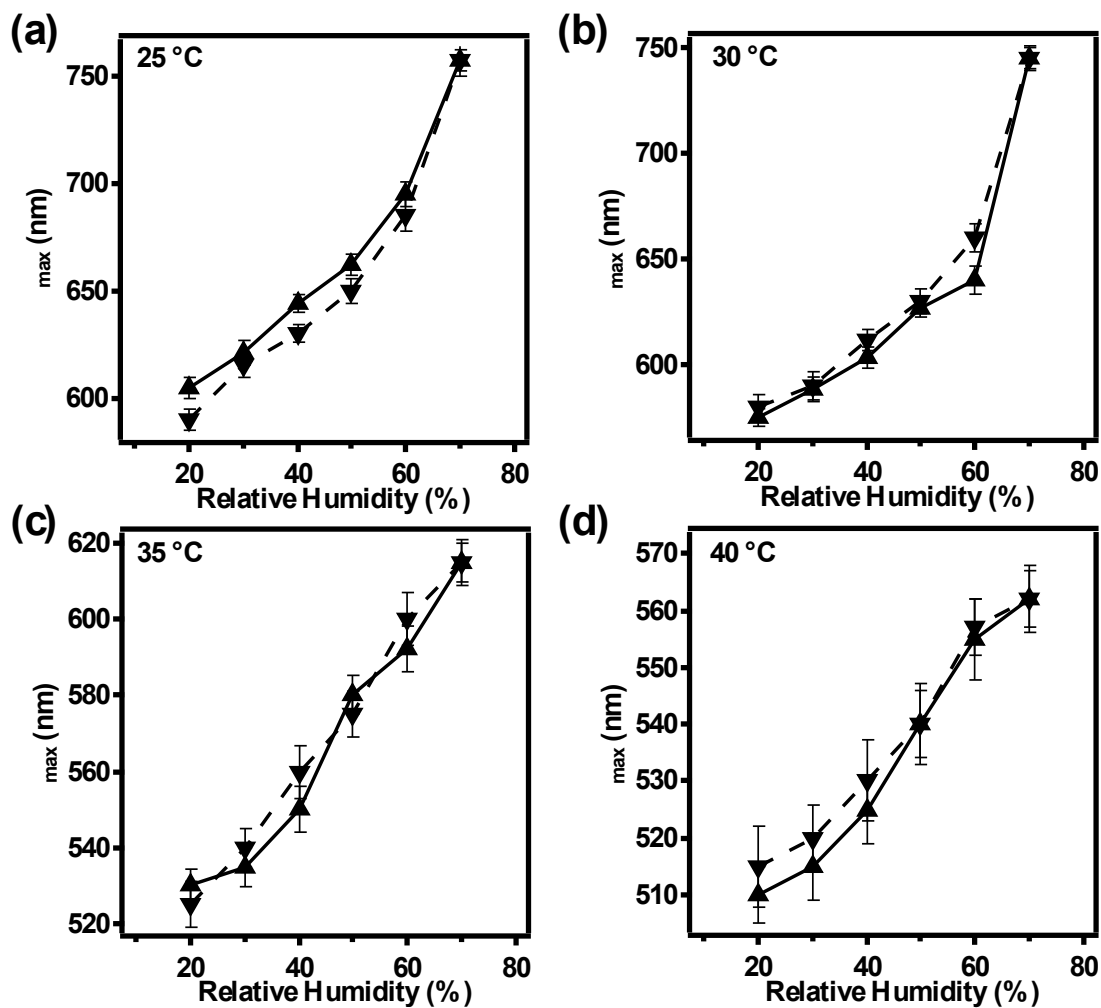


Fig 7. Position of a single reflectance peak ( $\lambda_{\max}$ ) for an etalon composed of microgels coated with pDADMAC/PSS/pDADMAC/PSS/pDADMAC at (a) 25 °C, (b) 30 °C, (c) 35 °C, and (d) 40 °C. Here, symbol (▲) indicates a humidity increase cycle while symbol (▼) denotes a humidity decrease cycle. Each data point represents the average of at least three independent measurements on the same device, and the error bars are the standard deviation for those values.

Finally, we were able to conclude that the sensitivity of the devices to humidity can be increased by layering the hygroscopic polyelectrolyte pDADMAC on the microgel layer prior to deposition of the final Au layer. The data is summarized in Table 1, which clearly shows devices with more pDADMAC layers are more sensitive to humidity.

**Table 1:** The table outlining the change in  $\Delta\lambda_{\max}$  for different devices at different temperature.

Device	Temperature, (°C)				
	25	30	35	40	
Etalon	112	57	82	43	$\Delta\lambda_{\max}$ Value
pDADMAC Etalon	138	98	42	43	
pDADMAC/PSS/pDADMAC Etalon	140	190	110	62	
pDADMAC/PSS/pDADMAC/PSS/pDADMAC	152	70	85	52	

**Conclusion:**

In summary, we were able to show that pNIPAm microgel-based etalons can be used as a humidity sensor over a wide range of humidity. Additional multilayers of polyelectrolytes can be added to the microgel layers to enhance the sensitivity of the devices to humidity. We attribute the increased sensitivity to the hygroscopic pDADMAC, which allows the microgel-based cavity to more extensively swell in humid air. We also showed that the response of the devices to humidity was reproducible over many humidity increase/decrease cycles with minimal hysteresis. Additionally, we investigated the response of the devices to humidity at various temperatures. The data showed that the

device response to humidity was more linear at elevated temperature, although the sensitivity of the devices to humidity was higher at low temperature. Finally, these devices are easy to fabricate and use, inexpensive, and do not require any special equipment to determine humidity — a simple color change detectable by eye can be related to humidity (although fine humidity determination would be a challenge in this case). We expect that the devices here can be made sensitive to other vapors by incorporating materials that selectively bind desired species of interest. The devices here can also be easily arrayed on substrates to potentially make a single device capable of sensing multiple vapors. These are clear advantages over commercially available technology, which yield only electronic signals, are considerably more expensive than the devices here, and are only sensitive to a single vapor (a new sensor is needed for each species of interest).

#### **Acknowledgements:**

MJS acknowledges funding from the University of Alberta (the Department of Chemistry and the Faculty of Science), the Natural Sciences and Engineering Research Council of Canada (NSERC), the Canada Foundation for Innovation (CFI), the Alberta Advanced Education & Technology Small Equipment Grants Program (AET/SEGP), Grand Challenges Canada and IC-IMPACTS.

#### **References:**

[1] B. Balakrishnan, R. Banerjee, Biopolymer-based hydrogels for cartilage tissue engineering, *Chem Rev*, 111 (2011) 4453-4474.

- [2] D.J. Beebe, J.S. Moore, J.M. Bauer, Q. Yu, R.H. Liu, C. Devadoss, B.H. Jo, Functional hydrogel structures for autonomous flow control inside microfluidic channels, *Nature*, 404 (2000).
- [3] M.A.C. Stuart, W.T.S. Huck, J. Genzer, M. Muller, C. Ober, M. Stamm, G.B. Sukhorukov, I. Szleifer, V.V. Tsukruk, M. Urban, F. Winnik, S. Zauscher, I. Luzinov, S. Minko, Emerging applications of stimuli-responsive polymer materials, *Nat Mater*, 9 (2010) 101-113.
- [4] E. Kokufata, Y.Q. Zhang, T. Tanaka, Saccharide-sensitive phase transition of a lectin-loaded gel, *Nature (London)*, 351 (1991) 302-304.
- [5] K. Tsujii, M. Hayakawa, T. Onda, T. Tanaka, A novel hybrid material of polymer gels and bilayer-membranes, *Trans. Mater. Res. Soc. Jpn.*, 26 (2001) 639-642.
- [6] A.B.W. Brochu, S.L. Craig, W.M. Reichert, Self-healing biomaterials, *J. Biomed. Mater. Res., Part A*, 96A (2011) 492-506.
- [7] J.M. Lenhardt, S.L. Craig, Force probes in a bottle, *Nat. Nanotechnol.*, 4 (2009) 284-285.
- [8] D.M. Loveless, N.I. Abu-Lail, M. Kaholek, S. Zauscher, S.L. Craig, Reversibly cross-linked surface-grafted polymer brushes, *Angew. Chem., Int. Ed.*, 45 (2006) 7812-7814.
- [9] L. Brunsveld, E.W. Meijer, R.B. Prince, J.S. Moore, Self-assembly of folded m-phenylene ethynylene oligomers into helical columns, *J Am Chem Soc*, 123 (2001) 7978-7984.
- [10] S.R. White, N.R. Sottos, P.H. Geubelle, J.S. Moore, M.R. Kessler, S.R. Sriram, E.N. Brown, S. Viswanathan, Autonomic healing of polymer composites. [Erratum to document cited in CA134:341243], *Nature (London, U. K.)*, 415 (2002) 817.

- [11] R. Pelton, Temperature-sensitive aqueous microgels, *Adv. Colloid Interface Sci.*, 85 (2000) 1-33.
- [12] W.H. Blackburn, E.B. Dickerson, M.H. Smith, J.F. McDonald, L.A. Lyon, Peptide-Functionalized Nanogels for Targeted siRNA Delivery, *Bioconjugate Chem.*, 20 (2009) 960-968.
- [13] T. Hoare, R. Pelton, Highly pH and Temperature Responsive Microgels Functionalized with Vinylacetic Acid, *Macromolecules*, 37 (2004) 2544-2550.
- [14] J. Kim, S. Nayak, L.A. Lyon, Bioresponsive Hydrogel Microlenses, *J. Am. Chem. Soc.*, 127 (2005) 9588-9592.
- [15] J. Kleinen, A. Klee, W. Richtering, Influence of Architecture on the Interaction of Negatively Charged Multisensitive Poly(N-isopropylacrylamide)-co-Methacrylic Acid Microgels with Oppositely Charged Polyelectrolyte: Absorption vs Adsorption, *Langmuir*, 26 (2010) 11258-11265.
- [16] W. Xu, Y. Gao, M.J. Serpe, Electrochemically color tunable poly(N-isopropylacrylamide) microgel-based etalons, *Journal of Materials Chemistry C*, 2 (2014) 3873-3878.
- [17] C. Dagallier, H. Dietsch, P. Schurtenberger, F. Scheffold, Thermoresponsive hybrid microgel particles with intrinsic optical and magnetic anisotropy, *Soft Matter*, 6 (2010) 2174-2177.
- [18] W. Richtering, A. Pich, The special behaviours of responsive core-shell nanogels, *Soft Matter*, 8 (2012) 11423-11430.
- [19] B.R. Saunders, Doubly crosslinked microgels, *Wiley-VCH Verlag GmbH & Co. KGaA*, 2012, pp. 141-167.

- [20] T. Hoare, R. Pelton, Functional Group Distributions in Carboxylic Acid-Containing Poly(N-isopropylacrylamide) Microgels, *Langmuir*, 20 (2004) 2123-2133.
- [21] H. Kanazawa, K. Yamamoto, Y. Matsushima, N. Takai, A. Kikuchi, Y. Sakurai, T. Okano, Temperature-responsive chromatography using poly(N-isopropylacrylamide)-modified silica, *Analytical Chemistry*, 68 (1996) 100-105.
- [22] M.J. Serpe, J. Kim, L.A. Lyon, Colloidal hydrogel microlenses, *Adv. Mater. (Weinheim, Ger.)*, 16 (2004) 184-187.
- [23] C. Wu, S.Q. Zhou, Internal motions of both poly(N-isopropylacrylamide) linear chains and spherical microgel particles in water, *Macromolecules*, 29 (1996) 1574-1578.
- [24] S. Nayak, H. Lee, J. Chmielewski, L.A. Lyon, Folate-mediated cell targeting and cytotoxicity using thermoresponsive microgels, *J. Am. Chem. Soc.*, 126 (2004) 10258-10259.
- [25] K. Kratz, T. Hellweg, W. Eimer, Influence of charge density on the swelling of colloidal poly(N-isopropylacrylamide-co-acrylic acid) microgels, *Colloids Surf., A*, 170 (2000) 137-149.
- [26] C.D. Sorrell, M.J. Serpe, Reflection Order Selectivity of Color-Tunable Poly(N-isopropylacrylamide) Microgel Based Etalons, *Adv. Mater.*, 23 (2011) 4088-4092.
- [27] K.K. Kanazawa, J.G. Gordon, II, The oscillation frequency of a quartz resonator in contact with a liquid, *Anal. Chim. Acta*, 175 (1985) 99-105.
- [28] M.R. Islam, M.J. Serpe, Label-free detection of low protein concentration in solution using a novel colorimetric assay, *Biosens. Bioelectron.*, 49 (2013) 133-138.

- [29] M.R. Islam, M.J. Serpe, Polyelectrolyte mediated intra and intermolecular crosslinking in microgel-based etalons for sensing protein concentration in solution, *Chem Commun*, 49 (2013) 2646-2648.
- [30] M.R. Islam, M.J. Serpe, Polymer-based devices for the label-free detection of DNA in solution: low DNA concentrations yield large signals, *Anal. Bioanal. Chem.*, 406 (2014) 4777-4783.
- [31] Y. Gao, G.P. Zago, Z. Jia, M.J. Serpe, Controlled and Triggered Small Molecule Release from a Confined Polymer Film, *ACS Appl. Mater. Interfaces*, 5 (2013) 9803-9808.
- [32] D. Parasuraman, A.K. Sarker, M.J. Serpe, Poly(N-Isopropylacrylamide)-Based Microgels and Their Assemblies for Organic-Molecule Removal from Water, *ChemPhysChem*, 13 (2012) 2507-2515.
- [33] D. Parasuraman, M.J. Serpe, Poly(N-Isopropylacrylamide) Microgel-Based Assemblies for Organic Dye Removal from Water, *ACS Appl. Mater. Interfaces*, 3 (2011) 4714-4721.
- [34] M.R. Islam, M.J. Serpe, Penetration of Polyelectrolytes into Charged Poly(N-isopropylacrylamide) Microgel Layers Confined between Two Surfaces, *Macromolecules*, 46 (2013) 1599-1606.
- [35] M.R. Islam, X. Li, K. Smyth, M.J. Serpe, Polymer-Based Muscle Expansion and Contraction, *Angew. Chem., Int. Ed.*, 52 (2013) 10330-10333.
- [36] M.R. Islam, M.J. Serpe, Poly(N-isopropylacrylamide) microgel-based thin film actuators for humidity sensing, *RSC Adv.*, 4 (2014) 31937-31940.

[37] M. McCormick, R.N. Smith, R. Graf, C.J. Barrett, L. Reven, H.W. Spiess, NMR Studies of the Effect of Adsorbed Water on Polyelectrolyte Multilayer Films in the Solid State, *Macromolecules*, 36 (2003) 3616-3625.

[38] C.D. Sorrell, M.C.D. Carter, M.J. Serpe, A "Paint-On" Protocol for the Facile Assembly of Uniform Microgel Coatings for Color Tunable Etalon Fabrication, *ACS Appl. Mater. Interfaces*, 3 (2011) 1140-1147.

[39] M. Unemori, Y. Matsuya, S. Matsuya, A. Akashi, A. Akamine, Water absorption of poly(methyl methacrylate) containing 4-methacryloxyethyl trimellitic anhydride, *Biomaterials*, 24 (2003) 1381-1387.